

Dalton Transactions

Accepted Manuscript



This is an *Accepted Manuscript*, which has been through the Royal Society of Chemistry peer review process and has been accepted for publication.

Accepted Manuscripts are published online shortly after acceptance, before technical editing, formatting and proof reading. Using this free service, authors can make their results available to the community, in citable form, before we publish the edited article. We will replace this *Accepted Manuscript* with the edited and formatted *Advance Article* as soon as it is available.

You can find more information about *Accepted Manuscripts* in the [Information for Authors](#).

Please note that technical editing may introduce minor changes to the text and/or graphics, which may alter content. The journal's standard [Terms & Conditions](#) and the [Ethical guidelines](#) still apply. In no event shall the Royal Society of Chemistry be held responsible for any errors or omissions in this *Accepted Manuscript* or any consequences arising from the use of any information it contains.

ARTICLE

Theoretical Evidence of Metal-Induced Structural Distortions in a Series of Bipyrimidine-Based Ligands

Cite this: DOI: 10.1039/x0xx00000x

Camille Latouche,^a Huriye Akdas-Kilig*,^b Jean-Pierre Malval,^c Jean-Luc Fillaut,^b Abdou Boucekkine*,^b Vincenzo Barone*^aReceived 00th January 2014,
Accepted 00th January 2014

DOI: 10.1039/x0xx00000x

www.rsc.org/

Herein, we report theoretical evidences of the geometric changes occurring upon complexation, for a series of octupolar bipyrimidine-based ligands incorporating NPh₂ terminal donor group. It is shown that ligands **1** and **2** (4,4',6,6'-Tetrakis(N,N-diphenylaminostyryl)-[2,2']bipyrimidine and 4,4',6,6'-Tetrakis((N,N-diphenyl)-9,9'-dioctyl-9H-fluorene-2-amine)-2,2'-bipyrimidine) exhibit a non-planar geometry with a torsion angle between both pyrimidine moieties of ~ 25° and 50° respectively. **1a** (complex of **1**) becomes planar upon addition of ZnCl₂ to the bipyrimidine moiety whereas **2a** remains distorted. Furthermore, an assignment of the absorption bands for all compounds is presented.

Introduction

Chromophores with large Stokes Shift and strong two photon absorption (TPA) have attracted a considerable amount of research thanks to their high potential of applications not only in several technological fields such as data storage^{1,2} and multi-dimensional microfabrication,³⁻⁷ but also for medical therapy.⁸ In the previous decade, quadratic Non Linear Optical (NLO) properties of octupolar tetrahedral D_{2d} and octahedral late metal complexes (D_3) with large π -donor backbones have been investigated.^{4,9,10} The idea of using bipyrimidine ligands arose for different reasons: (i) strong π -delocalization, (ii) non planarity between two bipyrimidine moieties promoted by lone pair's interactions between the nitrogen atoms of the two pyrimidine fragments, which gives access to a pseudo-tetrahedral octupolar symmetry and (iii) strong ability to chelate a metal and possibly give a supra-molecular assembly.¹¹⁻¹⁸

Recently, a new class of three-dimensional NLO-phores of D_{2d} symmetry based on donor-substituted styryl bipyrimidine cores has been investigated.⁹ Such derivatives exhibit interesting fluorescence and fluoro-solvatochromic properties, as well as large cubic and quadratic NLO responses, which can be tuned by the nature of the substituents within the styryl fragments. The photophysical properties of such compounds and materials are highly dependent on the adopted structure. In particular, a recent experimental paper by Malval *et al*¹⁹ on the two compounds sketched in Figure 1 reports that, upon addition of Zn²⁺, the overall structure of **1** becomes planar, whereas **2** retains a pseudo-tetrahedral shape. This arrangement was assumed to strongly impact the NLO properties of these bipyrimidine-based systems since the planarity of **1a** (*i.e.* the

complex of **1** with ZnCl₂) leads to the decrease of the TPA cross-section whereas the three-dimensional character of **2a** (*i.e.* the complex of **2** with ZnCl₂) promotes a strong enhancement of the TPA characteristics.

In the present study, a robust, easily reproducible, and efficient computational strategy has been employed to characterize the structures and spectroscopic features of the multi-branched zinc-bipyrimidine compounds introduced in ref.¹⁹ by means of methods rooted into the Density Functional Theory (DFT) and its time dependent extension (TD-DFT) coupled to a molecular mechanics (MM) description of more distant inert moieties and to a continuum description of bulk solvent effects by means of the polarizable continuum model (PCM). This work was performed in order to gain further insights about the planarization of the structure upon complexation by Zn.¹⁹

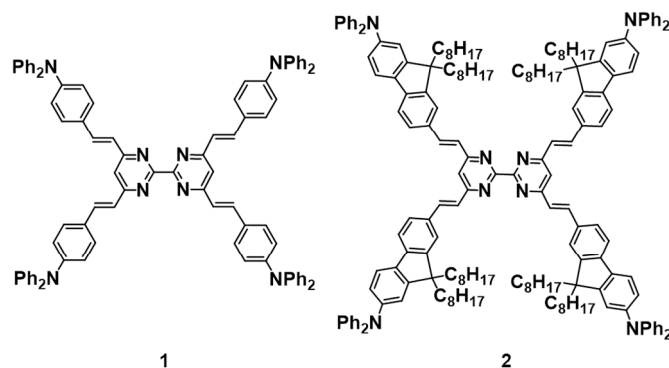


Figure 1. Studied compounds before complexation

Computational Details

All calculations have been carried out at the DFT level of theory with a development version of the Gaussian suite of programs.²⁰ The PBE0^{21,22} hybrid functional in conjunction with the 6-31G(d) basis set²³⁻²⁶ has been used to optimize geometries and to perform analytical frequency calculations. Electronic absorption calculations have been performed on the previous optimized geometries at the TD-DFT level with both PBE0 and CAM-B3LYP (CAM)²⁷ functionals. The whole **1** and **1a** (*i.e.* the complex **1** with ZnCl₂) systems have been treated by those quantum mechanical (QM) methods. Instead, for **2** and **2a** (*i.e.* the complex of **2** with ZnCl₂), an ONIOM strategy has been used in which the C₈H₁₇ moiety is described by the UFF force field,^{28,29} whereas the backbone (possibly including the ZnCl₂ moiety in **2a**) is treated at the DFT level. Solvent effects (specifically tetrahydrofuran, THF) have been taken into account at the default PCM level.^{30,31} MOs composition has been established thanks to the AOMix software.³² All spectra have been plotted by VMS-Draw.³³

Results and discussion

We start the discussion from the structures of **1** and **2**. The minimum on the Potential Energy Surface (PES) of **1** has *D*₂ symmetry, whereas the optimized structure of **2** which does not display any symmetry (Figure 2a) exhibits two different values for the torsional angles. As shown in Figure 2b and in Table 1, the torsion angle between both pyrimidines is larger for **2** than for **1** (24° and 49(46)° for **1** and **2** respectively) due to the strong steric hindrance of the C₈H₁₇ alkyl chains. This result is in good agreement with the X-ray torsional angle (36° with -NEt₂ moiety) reported by one of us.⁹ Moreover, the dihedral angle between two NPh₂, which represents better the torsion of the ligand, is also higher for **2** than for **1** (24° and 75(32)°, for **1** and **2** respectively). These results confirm the non-planar structure of both compounds in line with the quadratic NLO properties characteristic of a pseudo-tetrahedral shape.

Table 1. Relevant geometric data of **1** and **2**

	1	2
N ₁ -C-C-N ₂ (°)	24	45/49
N _a -C _b -C _c -N _d (°)	24	74/32

Figure 2. (a) Structural pictures of **1** and **2**. Hydrogen atoms have been omitted in **2** for clarity. (b) Dihedral angle of interest for the planarity of the studied compounds.

Upon addition of ZnCl₂, it turns out that complex **1a** becomes almost planar with N₁-C-C-N₂ and N_a-C_b-C_c-N_d torsion angles

close to 0°. On the other hand, complex **2a** does not exhibit such a quasi-planar conformation. The N₁-C-C-N₂ dihedral angle is nearly halved upon complexation (49(45)° vs. 23(26)° for **2** and **2a**, respectively). Furthermore, the N_a-C_b-C_c-N_d angle remains of the same order of magnitude than before complexation (74(32)° vs. 68(31)°) and is indicative of a strong torsion between the alkyl parts of the bipyrimidine ligand (Table 2). As assumed in the previous work and explicitly computed here, the structures of **2** and **2a** are different from **1** and **1a**.¹⁹ Therefore deeper investigations of those molecules have been performed; we now discuss and compare the electronic structure and the electronic absorption of the target compounds. As one can see in Figure 3, the HOMO-LUMO gaps of **1** and **2** are higher than their respective complexes (**1** and **1a**: 3.25 eV vs. 2.81 eV; **2** and **2a**: 3.08 eV vs. 2.60 eV). This difference is due to a non-negligible stabilization (ca. 0.5 eV) of the lowest unoccupied molecular orbitals (LUMOs), whereas the highest occupied molecular orbitals (HOMOs) are barely affected by the presence of the metal.

Table 2. Selected geometrical parameters of **1a** and **2a**

	1a	2a
Zn-N (Å)	2.055/2.046	2.037/2.067
Zn-Cl (Å)	2.274/2.273	2.264/2.277
N ₁ -C-C-N ₂ (°)	2/2	23/26
N _a -C _b -C _c -N _d (°)	0/3	68/31

The HOMOs of **1** (See ESI) are mainly localized on the donating group (56-61 % on NPh₂) reinforced by a strong localization on the π-chain (34-40 %) (Table 3). As expected, the LUMOs are less localized on the NPh₂ moieties (<10 %) and more concentrated on the bipyrimidine moiety, in particular LUMO, LUMO+1 and LUMO+2, (39-64%), thanks to its strong withdrawing character. Furthermore, the π-chain is still strongly involved in the LUMO.

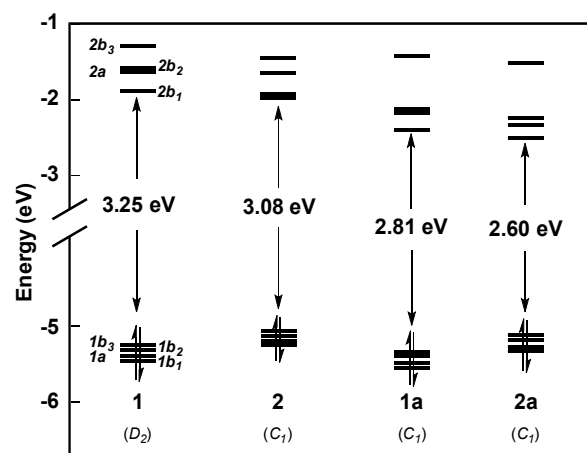


Figure 3. Energy levels of the studied compounds (PBE0/6-31G(d)).

Finally, it is noteworthy that the nitrogen atoms on the bipyrimidine play an important role and contribute strongly to the LUMO (20 %), LUMO+1 (20 %) and LUMO+2 (13 %). In the last orbital, the involvement of the C-C link between both

pyrimidines is also significant (17 %). The composition of the HOMOs is quite similar in the ligand **1** and in the complex **1a**. However, one should notice that the bipyrimidine moiety offers a larger contribution to the LUMOs of **1a** (55 %, 44 %, 67 % vs. 42 %, 39 %, 64 % for **1a** and **1**, respectively).

This increase of localization on the bipyrimidine moiety explains the stabilization of the LUMOs in the complex and the corresponding decrease of the HOMO-LUMO gap.

Furthermore, in analogy with **1**, the LUMO, LUMO+1 and LUMO+2 of **1a** exhibit a strong nitrogen character; in addition the latter orbital shows also a strong C-C character at the junction of the two bipyrimidines. The same trend is observed for **2** and **2a**, namely a strong localization of the HOMOs on the NPh₂ moieties, and of the LUMOs on the bipyrimidine and the π -chain (see ESI). Finally, as one can see in Table 3, the presence of the metal does not modify the localization of the frontier orbitals neither for **1a** nor for **2a**.

Table 3. Composition of the frontier orbitals (%).

	1			1a			
	Bpy	π_{chain}	NPh ₂	Bpy	π_{chain}	NPh ₂	ZnCl ₂
HOMO-3	5	34	61	5	33	62	0
HOMO-2	5	35	60	5	34	61	0
HOMO-1	4	40	56	4	40	56	0
HOMO	5	39	56	4	40	56	0
LUMO	42	53	5	55	40	4	1
LUMO+1	39	55	6	44	51	6	0
LUMO+2	64	33	3	67	30	3	0
LUMO+3	21	71	8	23	69	8	0

TD-DFT calculations have been performed with the PBE0 functional using the optimized geometries described above. As one can see in Table 4, the computed λ_{max} is always overestimated by ~75 nm, possibly due to the very long distance charge transfer associated with the transitions, from the NPh₂ moieties to bipyrimidine. Therefore, we decided to repeat the TD-DFT computations using a long-range corrected functional (CAM-B3LYP) able to reproduce correctly charge-transfer transitions. As one can observe in Table 4 and Figure 4, CAM-B3LYP slightly underestimates (by ~30-50 nm) the observed wavelengths of band maxima. Furthermore, in agreement with experiment, the calculations nicely reproduce the presence of two neighbouring absorption bands separated by ca. 30 nm.¹⁹

Our calculations give also information concerning the charge transfers within the different molecules. The absorption band of **1** is a mix of HOMO to LUMO+1 (31 %) and HOMO-1 to LUMO (35 %) transitions, which corresponds to a charge transfer from NPh₂ and π -chain to the core of the backbone, which includes the bipyrimidine and the π -chain moieties. The second absorption, computed at 359 nm, is more mixed. It turns out that the involved transitions are HOMO-3 to LUMO+1 (26 %), HOMO-2 to LUMO (33 %), HOMO-1 to LUMO+3 (14 %) and finally HOMO to LUMO+2 (13 %), and the charge transfer associated to the mixing of all those transitions from a NPh₂ and π -chain to the central backbone. The computed lowest energy absorption band of **2** slightly differs from that of **1** due

to the presence of two transitions in the same band (384 nm and 380 nm). The first electronic transition is from the HOMO to the LUMO (15 %) and to the LUMO+1 (24 %) with the same charge transfer as **1**. The second band is a large admixture from the frontier orbitals and the charge transfers associated to this band remains NPh₂ and π -chain to the central backbone. Upon addition of ZnCl₂, one can observe that the experimental redshift is nicely reproduced in the computations and the global trend is better reproduced using the PBE0 functional. Furthermore, as shown in the MOs diagram of **1a** and in Table 3, the ZnCl₂ moiety is not involved in the transitions. The computed and observed highest absorption bands exhibit a decrease of intensity when going from the free ligand to the complex. The first band of **1a**, computed at 422 nm, corresponds to a transfer mainly from HOMO-1 to LUMO (30 %) and from HOMO to LUMO+1 (26 %), analogous to the same charge transfer as the ligands. The second band computed at 387 nm corresponds to a transition from the HOMO-2 to the LUMO (42 %) and from the HOMO-3 to the LUMO+1 (23 %). In this latter case, the charge transfer occurs mainly from the NPh₂ moieties to bipyrimidine. Finally, **2a** (like **2**) exhibits two transitions in the highest absorption band (413 nm and 419 nm), which can be described as classical charge transfers from NPh₂ and π -chain toward the central backbone.

Table 4. Absorption wavelengths (nm) and oscillator strengths (f) of the studied compounds in THF.

	λ_{max}		
	PBE0	CAM-B3LYP	Exp ¹⁹
1	458 (f=2.7)	382 (f=3.7)	416
	431 (f=1.0)	359 (f=1.8)	
1a	527 (f=2.1)	422 (f=3.7)	459
	497 (f=0.5)	387 (f=1.8)	
	483 (f=0.6)		
2	474 (f=1.0)	384 (f=2.2)	423
	473 (f=2.6)	380 (f=3.8)	
	455 (f=0.4)	363 (f=0.9)	
2a	554 (f=0.4)	419 (f=1.8)	469
	552 (f=1.7)	413 (f=3.5)	
	531 (f=0.5)	387 (f=1.0)	
	522 (f=0.4)		

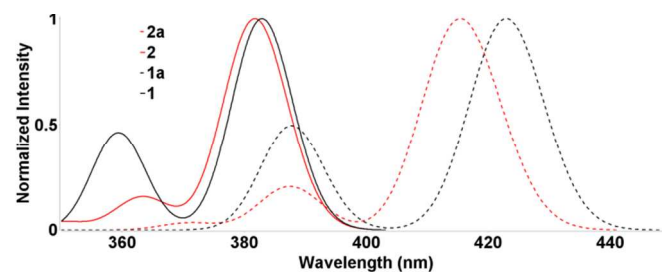


Figure 4. Simulated absorption spectra of **1** (black), **1a** (dashed black), **2** (red) and **2a** (dashed red). Intensities are normalized (CAM-B3LYP/6-31G(d)) (HWHM=400 cm⁻¹)

Moreover, the same absorption band at 387 nm has been computed for both **1a** and **2a**. However, in the latter case, this absorption band contains a large number of transitions, which globally correspond to the charge transfer from the frontier HOMOs to LUMO and LUMO+1 (see ESI).

Conclusions

In this paper, we have reported the essential results of a comprehensive structural and electronic investigation on two different bipyrimidine-based ligands and their complexes upon addition of ZnCl₂. DFT calculations have been performed showing quantitative agreement and evidences concerning the tetrahedral-shape of complexes **1a** and **2a**. Furthermore, our modelling confirms the hypothesis derived from experimental studies, namely that **1a** becomes planar, whereas **2a** remains distorted. In particular, the N_a-C_b-C_c-N_d and N₁-C-C-N₂ dihedral angles are almost equal to zero for **1a** whereas a strong distortion still appears for complex **2a**. Furthermore, TD-DFT computations allow an unbiased assignment of the absorption bands. In the next future, a deep investigation of the NLO properties and behaviour will be performed. Further studies on the same molecules will focus on their vibrational properties. Indeed, thanks to new computational developments,^{34,35} full (and, possibly, reduced dimensionality) perturbative anharmonic treatments could provide fruitful information and new clues concerning the behaviour of this class of compounds.

Acknowledgements

The research leading to these results has received funding from the European Union's Seventh Framework Programme (FP7/2007-2013) under grant agreement No. ERC-2012-AdG-320951-DREAMS. The authors gratefully thank the high-performance computer facilities of the DREAMS center (<http://dreamshpc.sns.it>) for providing computer resources. The support of the COST CMTS-Action CM1002 "CONvergent Distributed Environment for Computational Spectroscopy (CODECS)" is also acknowledged. The authors are grateful to GENCI-IDRIS and GENCI-CINES for an allocation of computing time (Grant No. 2013-080649).

Notes and references

^a Scuola Normale Superiore, Piazza dei Cavalieri 7, I-56126 Pisa, Italy

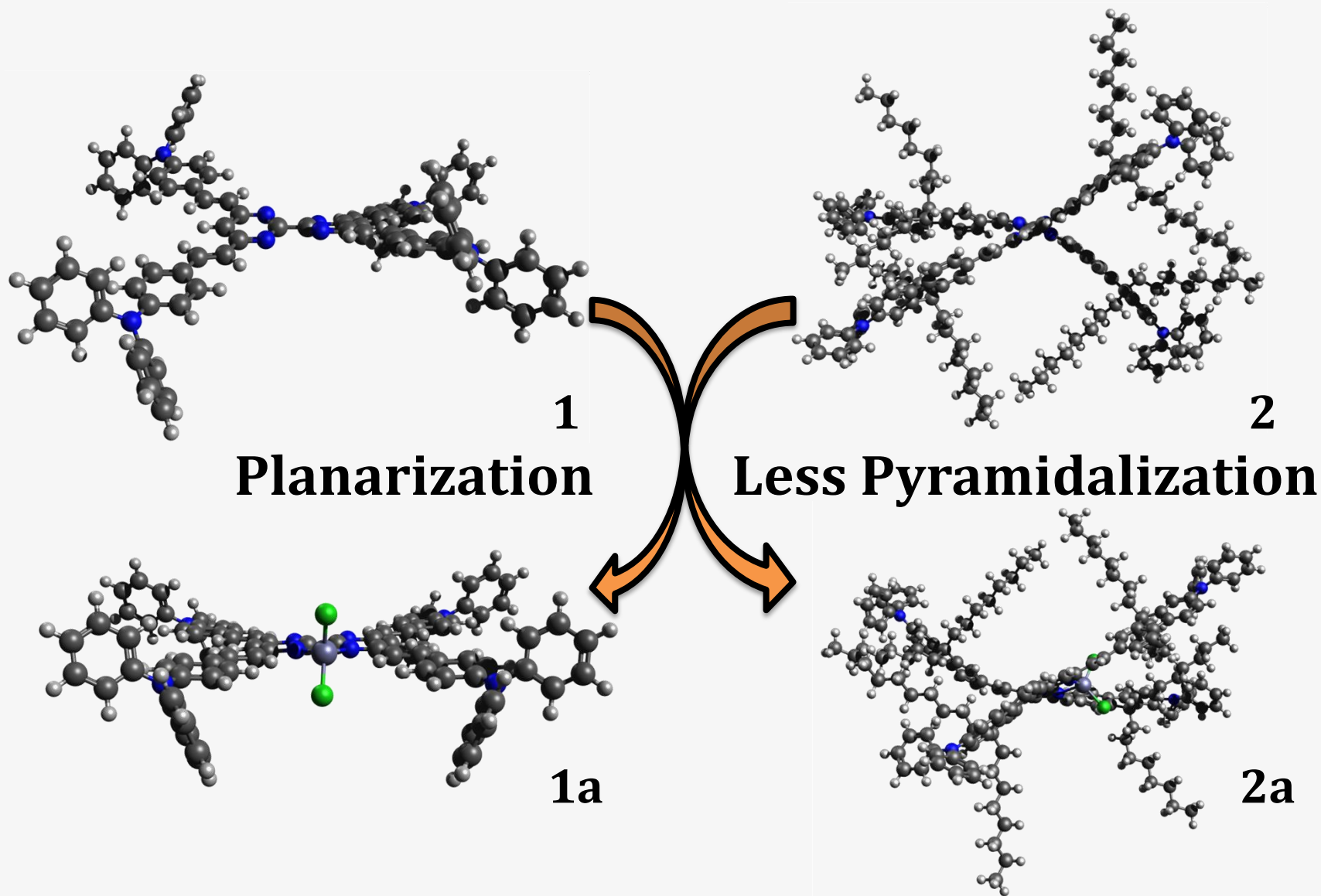
^b Institut des Sciences Chimiques de Rennes, UMR 6226 CNRS-Université de Rennes 1, Campus de Beaulieu, 35042 Rennes cedex, France.

^c Institut de Science des Matériaux de Mulhouse, UMR CNRS-UHA 7361, 15 rue Starcky - 68057 Mulhouse, France

Electronic Supplementary Information (ESI) available: 1) Electronic transition composition 2) MOs composition 3) Optimized geometric data

- W. Zhou, S. M. Kuebler, K. L. Braun, T. Yu, J. K. Cammack, C. K. Ober, J. W. Perry, and S. R. Marder, *Sci.*, 2002, **296**, 1106–1109.
- B. H. Cumpston, S. P. Ananthavel, S. Barlow, D. L. Dyer, J. E. Ehrlich, L. L. Erskine, A. A. Heikal, S. M. Kuebler, I.-Y. S. Lee, D. McCord-Maughon, J. Qin, H. Rockel, M. Rumi, X.-L. Wu, S. R. Marder, and J. W. Perry, *Nature*, 1999, **398**, 51–54.
- J.-P. Malval, F. Morlet-Savary, H. Chaumeil, L. Balan, D.-L. Versace, M. Jin, and A. Defoin, *J. Phys. Chem. C*, 2009, **113**, 20812–20821.
- J.-P. Malval, M. Jin, F. Morlet-Savary, H. Chaumeil, A. Defoin, O. Soppera, T. Scheul, M. Bouriau, and P. L. Baldeck, *Chem. Mater.*, 2011, **23**, 3411–3420.
- C. N. LaFratta, J. T. Fourkas, T. Baldacchini, and R. A. Farrer, *Angew. Chemie Int. Ed.*, 2007, **46**, 6238–6258.
- M. Jin, J.-P. Malval, D.-L. Versace, F. Morlet-Savary, H. Chaumeil, A. Defoin, X. Allonas, and J.-P. Fouassier, *Chem. Commun.*, 2008, 6540–6542.
- S. Kawata, H.-B. Sun, T. Tanaka, and K. Takada, *Nature*, 2001, **412**, 697–698.
- W. Denk, J. H. Strickler, and W. W. Webb, *Sci.*, 1990, **248**, 73–76.
- H. Akdas-Kilig, T. Roisnel, I. Ledoux, and H. Le Bozec, *New J. Chem.*, 2009, **33**, 1470–1473.
- L. Ordroneau, V. Aubert, V. Guerschais, A. Boucekkine, H. Le Bozec, A. Singh, I. Ledoux, and D. Jacquemin, *Chem. – A Eur. J.*, 2013, **19**, 5845–5849.
- K. J. H. Young, S. K. Meier, J. M. Gonzales, J. Oxgaard, W. A. Goddard, and R. A. Periana, *Organometallics*, 2006, **25**, 4734–4737.
- P. N. W. Baxter, G. S. Hanan, and J.-M. Lehn, *Chem. Commun.*, 1996, 2019–2020.
- K. D. Benkstein, C. L. Stern, K. E. Splan, R. C. Johnson, K. A. Walters, F. W. M. Vanhelmont, and J. T. Hupp, *Eur. J. Inorg. Chem.*, 2002, **2002**, 2818–2822.
- D. Armentano, G. de Munno, F. Lloret, M. Julve, J. Curely, A. M. Babb, and J. Y. Lu, *New J. Chem.*, 2003, **27**, 161–165.
- T. Lazarides, H. Adams, D. Sykes, S. Faulkner, G. Calogero, and M. D. Ward, *Dalt. Trans.*, 2008, 691–698.
- E. Riesgo, Y.-Z. Hu, F. Bouvier, and R. P. Thummel, *Inorg. Chem.*, 2001, **40**, 2541–2546.
- S. Swavey, J. A. Krause, D. Collins, D. D'Cunha, and A. Fratin, *Polyhedron*, 2008, **27**, 1061–1069.
- Q.-D. Liu, R. Wang, and S. Wang, *Dalt. Trans.*, 2004, 2073–2079.
- P. Savel, H. Akdas-Kilig, J.-P. Malval, A. Spangenberg, T. Roisnel, and J.-L. Fillaut, *J. Mater. Chem. C*, 2014, **2**, 295–305.
- M. J. Frisch, G. W. Trucks, H. B. Schlegel, G. E. Scuseria, M. A. Robb, J. R. Cheeseman, G. Scalmani, V. Barone, B. Mennucci, G. A. Petersson, H. Nakatsuji, M. Caricato, X. Li, H. R. Hratchian, A. F. Izmaylov, J. Bloino, G. Zheng, J. L. Sonnenberg, M. Hada, M. Ehara, K. Toyota, R. Fukuda, J. Hasegawa, M. Ishida, T. Nakajima, Y. Honda, O. Kitao, H. Nakai, T. Vreven, J. R. Montgomery Jr. J. A. Peralta, F. Ogliaro, M. Bearpark, J. J. Heyd, E. Brothers, K. N. Kudin, V. N. Staroverov, R. Kobayashi, J. Normand, K. Raghavachari, A. Rendell, J. C. Burant, S. S. Iyengar, J. Tomasi, M. Cossi, N. Rega, J. M. Millam, M. Klene, J. E. Knox, J. B. Cross, V. Bakken, C. Adamo, J. Jaramillo, R. Gomperts, R. E. Stratmann, O. Yazyev, A. J. Austin, R. Cammi, C. Pomelli, J. W. Ochterski, R. L. Martin, K. Morokuma, V. G. Zakrzewski, G. A. Voth, P. Salvador, J. J. Dannenberg, S. Dapprich, A. D. Daniels, O. Farkas, J. B. Foresman, J. V. Ortiz, J. Cioslowski, and D. J. Fox, 2013, G01303000.
- C. Adamo and V. Barone, *J. Chem. Phys.*, 1999, **110**, 6158–6169.
- M. Ernzerhof and G. E. Scuseria, *J. Chem. Phys.*, 1999, **110**, 5029–5036.
- V. A. Rassolov, J. A. Pople, M. A. Ratner, and T. L. Windus, *J. Chem. Phys.*, 1998, **109**, 1223–1229.
- M. M. Francl, W. J. Pietro, W. J. Hehre, J. S. Binkley, M. S. Gordon, D. J. DeFrees, and J. A. Pople, *J. Chem. Phys.*, 1982, **77**, 3654–3665.
- J. D. Dill and J. A. Pople, *J. Chem. Phys.*, 1975, **62**, 2921–2923.
- W. J. Hehre, R. Ditchfield, and J. A. Pople, *J. Chem. Phys.*, 1972, **56**, 2257–2261.
- T. Yanai, D. P. Tew, and N. C. Handy, *Chem. Phys. Lett.*, 2004, **393**, 51–57.
- T. Vreven, K. Morokuma, Ö. Farkas, H. B. Schlegel, and M. J. Frisch, *J. Comput. Chem.*, 2003, **24**, 760–769.
- S. Dapprich, I. Komáromi, K. S. Byun, K. Morokuma, and M. J. Frisch, *J. Mol. Struct. THEOCHEM*, 1999, **462**, 1–21.
- M. Cossi, G. Scalmani, N. Rega, and V. Barone, *J. Chem. Phys.*, 2002, **117**, 43.
- V. Barone, M. Cossi, and J. Tomasi, *J. Chem. Phys.*, 1997, **107**, 3210.
- S. I. Gorelsky, *AOMix: Program for Molecular Orbital Analysis*, 2009.
- D. Licari, A. Baiardi, M. Biczysko, F. Egidi, C. Latouche, and V. Barone, *J. Comput. Chem.*, 2014, 10.1002/jcc.23785.
- C. Latouche, F. Palazzetti, D. Skouteris, and V. Barone, *J. Chem. Theory Comput.*, 2014, **10**, 4565–4573.
- A. Baiardi, C. Latouche, J. Bloino, and V. Barone, *Dalt. Trans.*, 2014, **Accepted**, DOI: 10.1039/C4DT02151G.

EXPERIMENTALLY SUPPOSED



... **CONFIRMED BY DFT**